Analytical Model of the Wire-Bonded Interdigital Capacitor

Enrique Márquez-Segura, *Member, IEEE*, Francisco P. Casares-Miranda, *Student Member, IEEE*, Pablo Otero, *Member, IEEE*, Carlos Camacho-Peñalosa, *Member, IEEE*, and Juan E. Page

***Abstract*—The wire-bonded interdigital capacitor (WBIDC) is an interdigital capacitor with short circuits across the end of alternate fingers that result in an improved frequency response. This paper presents the analytical and circuital models of the WBIDC, which are useful to design and to incorporate into an electromagnetic or circuit analysis computer-aided design program. Design equations of the WBIDC are also presented. The analytical model and design equations have been validated with numerical analysis and experimental work.**

***Index Terms*—Interdigital capacitor (IDC), microwave passive circuits, wire-bonded interdigital capacitor (WBIDC), wire bonding.**

I. Introduction

MICROSTRIP circuits using composite right/left-handed transmission lines (CRLH-TLs) [1], [2] need series capacitors to operate at frequencies beyond the resonant frequencies of printed interdigital capacitors (IDCs). Recently, an enhanced IDC, the so-called wire-bonded interdigital capacitor (WBIDC), which is basically an IDC with short circuits across the end of alternate fingers, has been presented [3]. Microstrip IDC and WBIDC are shown in Fig. 1(a) and (b), respectively. The improvement of the WBIDC over the IDC is due to the bonding wires, which eliminate the above-mentioned resonances.

The WBIDC can be analyzed with the help of an electromagnetic (EM) computer-aided design (CAD) program. If printed, the best choice is an EM solver based on the integral equation and the method of moments. In that case, the bonding wires are introduced in the program by means of vertical *vias* from the finger ends to a second trace layer placed above the IDC through an air layer. The vertical *vias* are then connected among themselves on that second trace layer, i.e., the analysis of a WBIDC is a cumbersome task because the WBIDC has to be drafted and the simulation time is long. Any simple geometrical modification means that the WBIDC has to be redrafted and analyzed again. Hence, an accurate analytical model of the WBIDC would be very welcome.

Manuscript received July 31, 2005; revised October 5, 2005. This work was supported by the Spanish Ministry of Science and Technology and by the European Regional Development Funds of the European Union under Grant TIC2003-05027.

E. Márquez-Segura, F. P. Casares-Miranda, Pablo Otero, and C. Camacho-Peñalosa are with the Departamento Ingeniería de Comunicaciones, Escuela Técnica Superior de Ingeniería de Telecomunicación, Universidad de Málaga, 29071 Málaga, Spain (e-mail: casares@ic.uma.es).

J. E. Page is with the Departamento Electromagnetismo y Teoría de Circuitos, Escuela Técnica Superior de Ingeniería de Ingenieros de Telecomunicación, Universidad Politécnica de Madrid, 28040 Madrid, Spain.

Digital Object Identifier 10.1109/TMTT.2005.862634

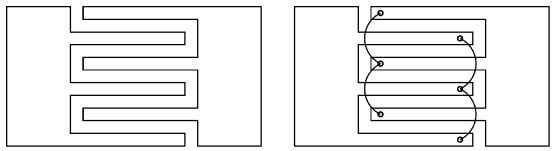

Fig. 1. (a) IDC. (b) WBIDC.

In this paper, a simplified analytical model of the WBIDC, ready to be incorporated into an EM or circuit analysis CAD program, is developed. Section II shows how the analytical model is developed. Design formulas, derived from the model, are presented in Section III-A. Compact formulas allow circuit designers to calculate any required WBIDC. Section III-A also presents an equivalent two-port circuit, valid at low frequencies, of the WBIDC. The analysis has been done first neglecting losses. Second, the quality factor Q of the WBIDC has been calculated as well, as described in Section III-B. The model and design formulas are validated with the numerical simulations and the experiments presented in Section IV. Finally, the effect of the inductance of the bonding wires has been studied in Section V.

II. Analytical Model

The structure of a simple printed IDC is shown in Fig. 1(a). This circuit shows a number of resonant frequencies that limit the operational bandwidth of the IDC. Fig. 1(b) shows a microstrip WBIDC. When the bonding wires are connected, those resonances disappear [3].

The transmission-line equivalent of a Lange coupler is shown in Fig. 2. The Lange coupler and WBIDC are different circuits. The former is a four-port circuit, the length of the fingers being a quarter wavelength and is used to couple part of the energy present at one port to two other ports. The later is a two-port device that emulates a capacitance and the fingers can have any length, usually less than a quarter wavelength. Nevertheless, from the circuital point-of-view and with the only purpose of analysis, the WBIDC can be considered to be a Lange coupler of any length and with ports 2 and 4 open ended. When losses are neglected and coupling between nonadjacent lines is negligible, the admittance matrix of the Lange coupler is [4]

$$[Y_L] = \begin{bmatrix} -jM\cot\theta & -jN\cot\theta & jN\csc\theta & jM\csc\theta \\ -jN\cot\theta & -jM\cot\theta & jM\csc\theta & jN\csc\theta \\ jN\csc\theta & jM\csc\theta & -jM\cot\theta & -jN\cot\theta \\ jM\csc\theta & jN\csc\theta & -jN\cot\theta & -jM\cot\theta \end{bmatrix} \quad (1)$$

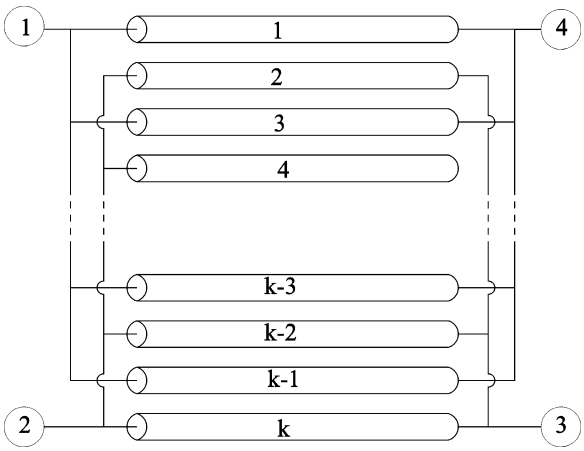

Fig. 2. Lange coupler.

where θ is the electrical length of the fingers and

$$M = \frac{k}{2}Y_{11} + \left(\frac{k}{2} - 1\right)\frac{Y_{12}^2}{Y_{11}} \tag{2a}$$

$$N = (k-1)Y_{12} \tag{2b}$$

where k is the number of fingers, which is even, and

$$Y_{11} = \frac{1}{2}(Y_{oo} + Y_{oe}) \tag{3a}$$

$$Y_{12} = -\frac{1}{2}(Y_{oo} - Y_{oe}). \tag{3b}$$

The admittances Y_{oe} and Y_{oo} in (3) are the even- and odd-mode admittances, respectively, of a pair of adjacent fingers of the coupler. When no losses are considered, admittances Y_{oe} and Y_{oo} are real numbers. It happens that $Y_{oo} > Y_{oe}$ [5]. From (2) and (3), it is then easy to demonstrate that $N < 0, M > 0$, and $M^2 > N^2$ [4].

The corresponding impedance matrix is obtained inverting matrix (1) as follows:

$$[Z_L] = \frac{1}{N^2 - M^2} \times \begin{bmatrix} jM\cot\theta & -jN\cot\theta & -jN\csc\theta & jM\csc\theta \\ -jN\cot\theta & jM\cot\theta & jM\csc\theta & -jN\csc\theta \\ -jN\csc\theta & jM\csc\theta & jM\cot\theta & -jN\cot\theta \\ jM\csc\theta & -jN\csc\theta & -jN\cot\theta & jM\cot\theta \end{bmatrix}. \tag{4}$$

When currents in ports 2 and 4 are zero (because they are open ended), the resulting two-port circuit is a WBIDC, and its impedance matrix is

$$[Z_W] = \frac{1}{N^2 - M^2}\begin{bmatrix} jM\cot\theta & -jN\csc\theta \\ -jN\csc\theta & jM\cot\theta \end{bmatrix}. \tag{5}$$

The impedance parameters in (5) can be easily converted to S-parameters using [6]

$$S_{11} = S_{22} = \frac{Z_{11}^2 - Z_{21}^2 - Z_0^2}{(Z_{11} + Z_0)^2 - Z_{21}^2} \tag{6a}$$

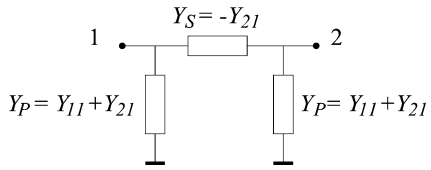

Fig. 3. Π-type two-port circuit.

$$S_{12} = S_{21} = \frac{2Z_{21}Z_0}{(Z_{11} + Z_0)^2 - Z_{21}^2} \tag{6b}$$

where Z_0 is the reference impedance. The matrix in (5) can be inverted again to obtain the admittance matrix of the WBIDC as follows:

$$[Y_W] = \frac{N^2 - M^2}{M^2\cos^2\theta - N^2} \times \begin{bmatrix} -jM\sin\theta\cos\theta & -jN\sin\theta \\ -jN\sin\theta & -jM\sin\theta\cos\theta \end{bmatrix}. \tag{7}$$

Matrices in (5)–(7) can be incorporated into any circuit analysis CAD program.

The presented analytical model, valid for a WBIDC with an even number of fingers, has a few limitations. First, the exact calculation of the admittances of a pair of coupled lines [Y_{oe} and Y_{oo} in (3)]. Second, losses and the coupling between nonadjacent lines have been neglected. Third, the bonding wires across alternate fingers have been considered ideal short circuits. Finally, as mentioned, the model has been developed for a WBIDC with an even number of fingers.

III. Design Formulas and Equivalent Circuit

A. Lossless Model

The Π equivalent circuit of a two-port circuit is shown in Fig. 3. If matrix (7) was the admittance matrix of this circuit, then

$$Y_S = j\frac{N\,(N^2 - M^2)\sin\theta}{M^2\cos^2\theta - N^2} \tag{8a}$$

$$Y_P = -j\frac{(N^2 - M^2)\sin\theta}{M\cos\theta - N}. \tag{8b}$$

An example of admittances Y_S and Y_P in (8a) and (8b) is shown in Fig. 4. The circuit in Fig. 3, along with the expressions in (8a) and (8b), are always valid no matter the electrical length of the fingers, i.e., the frequency range.

When fingers are electrically short, i.e., at frequencies where $\theta \ll 1$,

$$Y_S = -jN\theta \tag{9a}$$

$$Y_P = j(N + M)\theta. \tag{9b}$$

At very low frequencies, the two admittances Y_S and Y_P in (9a) and (9b) correspond to two capacitances C_0 and C_P, respectively, as can be seen in Fig. 4. The low-frequency equivalent circuit of the WBIDC is shown in Fig. 5. The low-frequency lumped parameters are C_0, C_P, L_S, and R_S. The elements L_S and R_S will be discussed at the conclusion of this section and

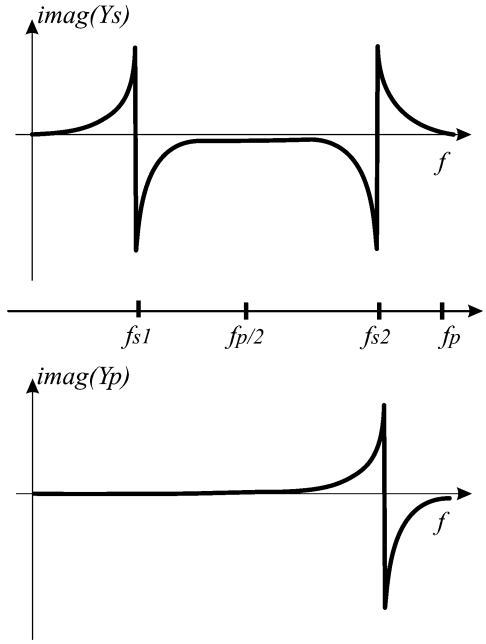

Fig. 4. Series and parallel susceptances $B_S = \mathrm{Imag}[Y_S]$ and $B_P = \mathrm{Imag}[Y_P]$.

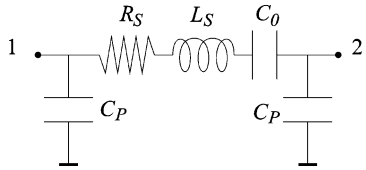

Fig. 5. Low-frequency equivalent circuit of the WBIDC (electrically short fingers).

in Section III-B, respectively. The two capacitances can be calculated as

$$C_0 = \frac{1}{2c}(k-1)d\sqrt{\varepsilon_{reff}}(Y_{oo} - Y_{oe}) \tag{10a}$$

$$C_P = \frac{1}{c}d\sqrt{\varepsilon_{reff}}\frac{[(k-1)Y_{oe} + Y_{oo}]Y_{oe}}{(Y_{oo} + Y_{oe})} \tag{10b}$$

where c is the speed of light, d is the length of the fingers, and the effective relative permittivity is computed from the corresponding values of the even and odd modes of a pair of adjacent fingers of the coupler [5]

$$\sqrt{\varepsilon_{reff}} = \frac{\sqrt{\varepsilon_{reffe}} + \sqrt{\varepsilon_{reffo}}}{2}. \tag{11}$$

The effective permittivity calculated with (11) gives a phase velocity that is the arithmetic mean of the phase velocities of the even and odd modes that propagate in the coupled lines. The validity of both the analytical model and equivalent circuit are limited by the exact calculation of the admittances of a pair of coupled lines, Y_{oe} and Y_{oo} in (3), as previously mentioned in Section II, but also by the exact calculation of the effective propagation characteristics of those coupled lines, which are reflected in the value of ε_{reff} in (11).

Above zero frequency, the first three singularities that presents the admittance Y_S in (8a) are two poles at frequencies where

$$\begin{aligned}\theta &= \theta_{S1,2} \\ &= \arccos\left(\mp\frac{N}{M}\right) \\ &= \arccos\left(\mp\frac{(k-1)(Y_{oe}^2 - Y_{oo}^2)}{(k-1)(Y_{oe}^2 + Y_{oo}^2) + 2Y_{oe}Y_{oo}}\right)\end{aligned} \tag{12}$$

and a zero at frequency where $\theta = \theta_P = \pi$. The two poles correspond to two zeros of series impedance, which means transmission. It is simple to realize that $\theta_{S2} = \pi - \theta_{S1}$. The two frequencies where this happens are

$$f_{S1} = \frac{c\theta_{S1}}{2\pi d\sqrt{\varepsilon_{reff}}} \tag{13a}$$

$$f_{S2} = \frac{c(\pi - \theta_{S1})}{2\pi d\sqrt{\varepsilon_{reff}}}. \tag{13b}$$

The condition $\theta = \pi$ means that the fingers are a half guided-wavelength long. The corresponding frequency is

$$f_P = \frac{c}{2d\sqrt{\varepsilon_{reff}}}. \tag{14}$$

At this frequency, there is no transmission between ports 1 and 2.

Between f_{Si}, $i = 1, 2$, and f_P (actually between f_{S1} and f_{S2}, as will be shown below), there is a frequency where the length of the fingers is a quarter guided wavelength, then $\theta = \pi/2$. The frequency where this happens is

$$f_{SR} = \frac{c}{4d\sqrt{\varepsilon_{reff}}} = \frac{f_P}{2}. \tag{15}$$

It is easy to demonstrate that the susceptance of Y_S is negative in the vicinity of f_{SR}, where it has a local maximum, as shown in Fig. 4, i.e., the series branch of the two-port circuit of Fig. 3 is highly reactive at f_{SR}, which means that there is no transmission. Considering the values that those different frequencies can take, it follows that

$$f_{S1} < f_{SR} = \frac{f_p}{2} < f_{S2} < f_P. \tag{16}$$

The frequency f_{S1} is the lowest series resonance frequency of the WBIDC. The series inductance L_S in Fig. 5 is obtained from that frequency as follows:

$$L_S = \frac{1}{4\pi^2 C_0 f_{S1}^2}. \tag{17}$$

It is important to note that the equivalent circuit of Fig. 5 is only valid up to frequency f_{S1}. Nevertheless, the design (10a), (10b), and (17) are extremely useful to design circuits using the WBIDC.

The exam of the admittance Y_P of (8b) also shows a pole at $\theta = \theta_{S2}$ and a zero at $\theta = \theta_P$, which correspond to frequencies f_{S2} and f_{SR}, respectively. These two frequencies are beyond the range where the proposed equivalent circuit of the WBIDC can be used.

Concerning the three frequencies f_{S1}, f_{SR}, and f_{S2}, the following discussion is of interest. There are two longitudinal

effects related to resonances. First, the series resonance of the combination of the finger inductances and the capacitances between fingers themselves and the capacitances to ground (f_{S1} and f_{S2}). Second, the longitudinal resonance, when the length of the fingers is a quarter guided wavelength (f_{SR}). For small values of C_0 (small number of fingers), the WBIDC stops being a capacitance and behaves as a series inductance above f_{S1}. When C_0 is made larger (more fingers are added), the turn-on frequency is between f_{S1} and f_{SR} and, when C_0 is made even larger, the turn-on frequency moves up to f_{SR}, the reason being the dependences of the admittance Y_S of (8a), that, in turn, are due to the influence of C_P in the circuit response because C_P grows with C_0. This point is very important if the WBIDC is used to build a CRLH-TL because the frequency response of the WBIDC is determinant to compute the frequency where the transmission line stops being left-handed and becomes right-handed [1].

B. Losses and Quality Factor

When losses are considered, the resistance R_S in the circuit of Fig. 5 is no longer zero. Its value is obtained as the real part of the impedance $Z_S = 1/Y_S$. The admittances in (8a) and (8b) are the lossless admittances. The expressions for Y_S and Y_P when losses are considered are

$$Y_S = \frac{N(N^2 - M^2)\sinh\gamma d}{M^2\cosh^2\gamma d - N^2} \tag{18b}$$

$$Y_P = -\frac{(N^2 - M^2)\sinh\gamma d}{M\cosh\gamma d - N} \tag{18b}$$

where $\gamma = \alpha + j\beta$ is the propagation constant of two adjacent fingers considered as a pair of coupled lines. The resistance of the series branch is then calculated as

$$R = \mathrm{Re}\left[\frac{1}{Y_S}\right] = \mathrm{Re}\left[\frac{M^2\cosh^2\gamma d - N^2}{N(N^2 - M^2)\sinh\gamma d}\right]. \tag{19}$$

At frequency f_{S1}, the series branch of the circuit in Fig. 5 resonates and the value of R_S is

$$R_S = R|_{f=f_{S1}}. \tag{20}$$

The quality factor of the WBIDC at a low-frequency f where the effect of L_S is negligible can be calculated as

$$Q = \frac{1}{2\pi f R_S C_0}. \tag{21}$$

IV. Model Validation

A. Numerical Validation

A WBIDC has been designed for a case study on a Rogers Ultralam 2000 substrate with relative permittivity 2.4 and thickness 1.52 mm (60 mil). Lines are 400-μm wide and gaps are 100 μm. The computed S-parameters in Fig. 6 are those of the circuit in Fig. 3 when Y_S and Y_P are the admittances of (8a) and (8b), respectively. The values of Y_{oe} and Y_{oo} have been computed using the expressions found in [7] and [8].

The previously mentioned behavior of the WBIDC with the number of fingers is shown in Fig. 6. Note that the case $k = 2$ corresponds to a pair of coupled lines. When the number of fingers is increased, the value of the series capacitance C_0 rises, but also the value of C_P does, as already explained in Section III. This effect depends on the relative permittivity of the substrate, on its thickness, and on the dimensions of the fingers and gaps.

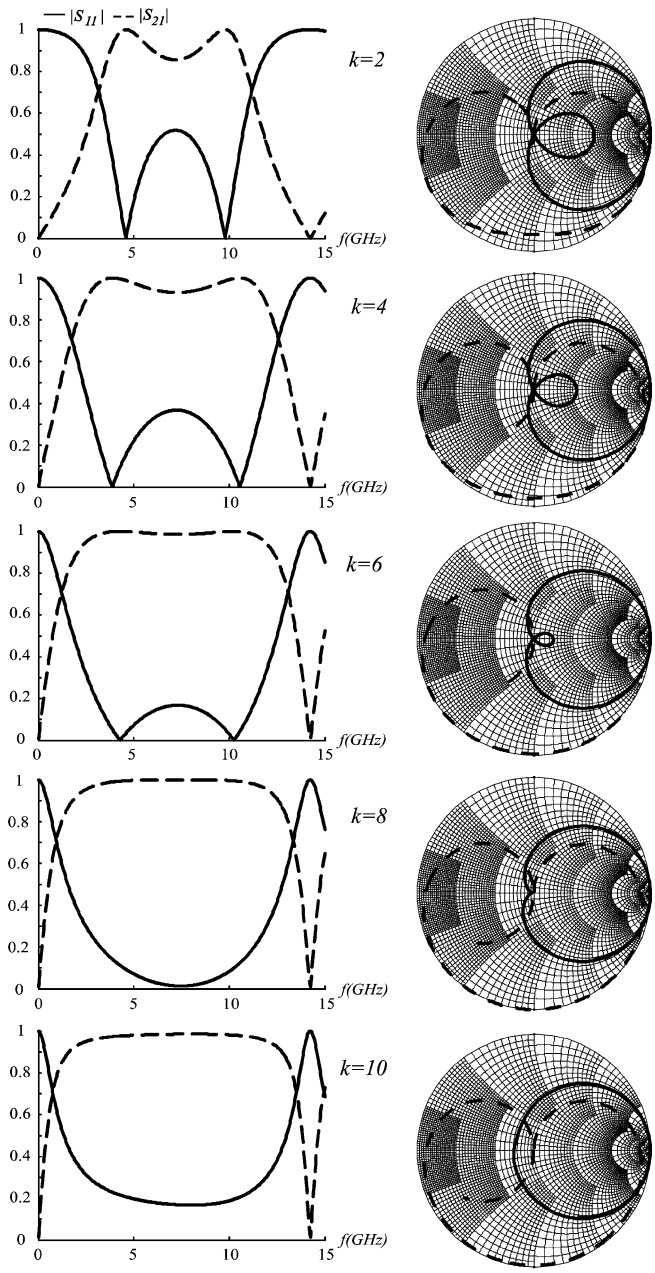

Fig. 6. S-parameters (reference impedance 50 Ω) of the WBIDC versus frequency, for a different number of fingers, computed from the circuit in Fig. 3 with (8a) and (8b).

TABLE I
LUMPED PARAMETERS VERSUS NUMBER OF FINGERS FOR THE WBIDC SHOWN IN FIG. 5. Q FACTOR CALCULATED AT 10 MHz

k	C_0 (pF)	C_P (pF)	L_S (nH)	R_S (Ω)	Q	f_{S1} (GHz)	f_{S2} (GHz)	f_P (GHz)
2	0.23	0.15	6.14	1.50	46K1	4.19	10.19	14.38
4	0.70	0.20	3.60	0.82	27K7	3.16	11.22	14.38
6	1.17	0.26	2.68	0.59	23K1	2.83	11.55	14.38
8	1.64	0.32	2.15	0.46	21K1	2.67	11.70	14.38

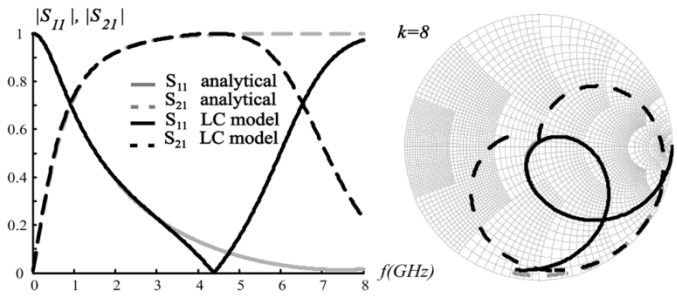

Fig. 7. S-parameters (reference impedance 50 Ω) of the WBIDC versus frequency, compared to its equivalent circuit (Fig. 5).

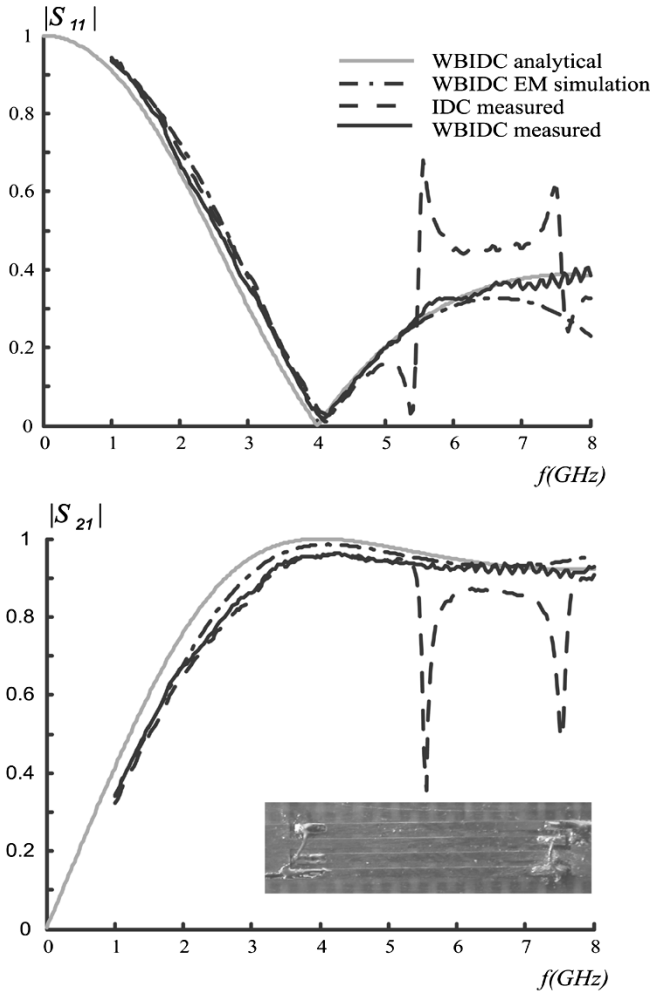

Fig. 8. Computed and measured S-parameters of the four-finger WBIDC prototype.

There is an optimal value of k for every combination of those parameters to obtain particularly good S-parameters (i.e., $k = 8$ in Fig. 6). Table I shows the values of the lumped elements of the equivalent circuit.

The response of the equivalent circuit of Fig. 5, compared to case $k = 8$ in Fig. 6, is shown in Fig. 7, where it can be seen that the equivalent circuit is only valid up to frequency f_{S1}, as already mentioned.

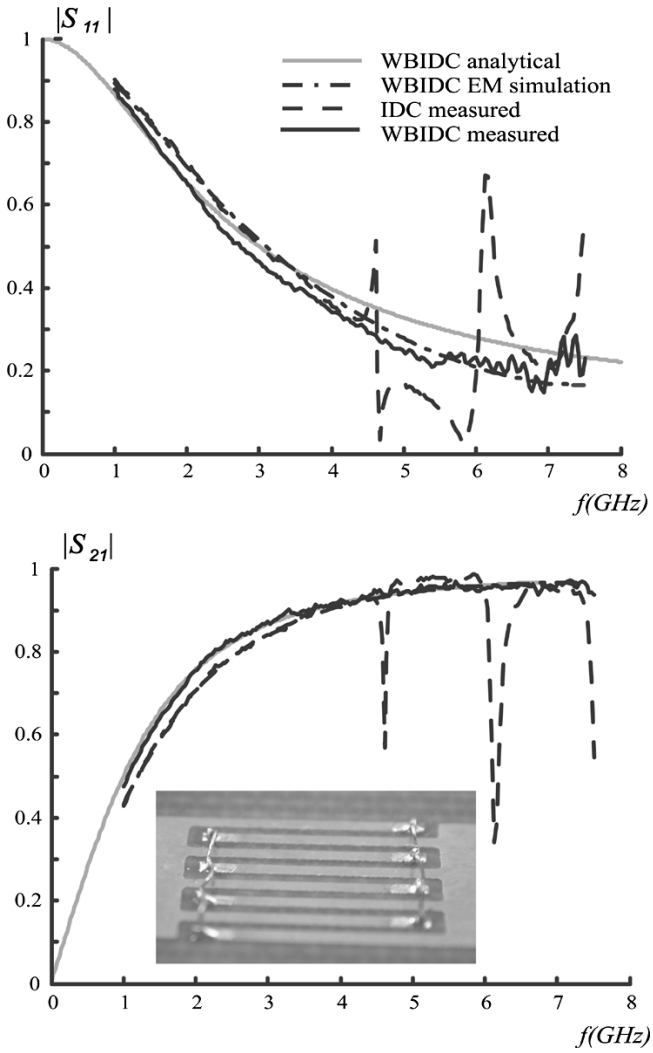

Fig. 9. Computed and measured S-parameters of the eight-finger WBIDC prototype.

B. Experimental Validation

The WBIDC and its analytical model have been validated with numerical simulation using a full-wave EM solver and with experimental work. Two WBIDC prototypes have been designed and printed on a Rogers Ultralam 2000 substrate, with relative permittivity of 2.4 and thickness of 1.52 mm (60 mil).

The first prototype has four fingers 8-mm long and 400-μm wide with gaps of 100 μm. Fig. 8 shows the simulated and measured S-parameters of this WBIDC. The second prototype has eight fingers 6.5-mm long and 410-μm wide, with gaps of 230 μm. The corresponding S-parameters are shown in Fig. 9. In both cases, the simulated parameters have been computed with the model of (6a) and (6b) ("WBIDC analytical" in Figs. 8 and 9) and Ansoft Ensemble ("WBIDC EM simulation" in Figs. 8 and 9). Measurements were carried out without and with the bonding wires (IDC and WBIDC, respectively) so that the benefits of using the latter are demonstrated as well. Figs. 8 and 9 show a very good agreement between the proposed analytical model and both the full-wave analysis and measurements.

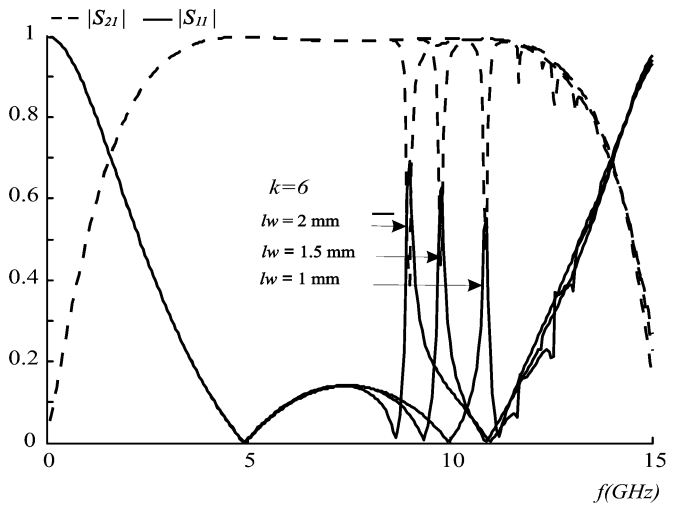

Fig. 10. S-parameters of the WBIDC versus frequency. Parameter the length of the bonding wire (lw).

V. Effect of Wire Inductance

The analytical model presented in this paper has several limitations that have been mentioned in Section II. The main difference between the IDC and WBIDC is the connection of alternate fingers with the bonding wires. The effect of the series inductances of the nonideal wires is an insignificant drawback of the WBIDC. These inductances give rise to a resonance of frequency close to frequency f_P. The higher the value of the wire inductance, the lower the frequency of that resonance. This effect can be observed in Fig. 10, where several wire lengths are considered for one of the cases analyzed in Section IV-A (six fingers printed on a Rogers Ultralam 2000 substrate with a relative permittivity of 2.4 and a thickness of 1.52 mm). It is important to mention that, for typical values of wire inductance, that resonance is out of the frequency range where the device behaves as a capacitor.

VI. Conclusion

In this paper, the analytical and circuital models of the WBIDC have been presented. The models allow to incorporate the WBIDC as a block into EM and circuit analysis CAD programs. The analytical model is accurate no matter the electrical length of the fingers, i.e., for any frequency. The circuital model is valid up to the frequency of series resonance of the WBIDC. Design equations of the WBIDC have been obtained from the analytical model. The analytical model and design equations have been validated with simulations using an EM solver based on the integral equation and the method of moments, and with experimental study. Agreement between the presented analytical model, the method of moments analysis, and the measurements results is very good.

The availability of the models and design equations presented in this paper makes the use of the WBIDC safe enough not only to design a CRLH-TL, but also in any design where a susceptance is needed with a performance superior to that of an IDC.

References

[1] A. Lai, C. Caloz, and T. Itoh, "Composite right/left-handed transmission line metamaterials," *IEEE Microw. Mag.*, vol. 5, no. 3, pp. 34–50, Sep. 2004.

[2] M. A. Antoniades and G. V. Eleftheriades, "Compact linear lead/lag metamaterial phase shifters for broad-band applications," *IEEE Antennas Wireless Propag. Lett.*, vol. 2, no. 1, pp. 103–106, Dec. 2003.

[3] F. P. Casares-Miranda, P. Otero, E. Márquez-Segura, and C. Camacho-Peñalosa, "Wire bonded interdigital capacitor," *IEEE Microw. Wireless Compon. Lett.*, vol. 15, no. 10, pp. 700–702, Oct. 2005.

[4] W. P. Ou, "Design equations for a interdigitated directional coupler," *IEEE Trans. Microw. Theory Tech.*, vol. MTT-23, no. 2, pp. 253–255, Feb. 1975.

[5] R. S. Elliott, *An Introduction to Guided Waves and Microwave Circuits*. Upper Saddle River, NJ: Prentice-Hall, 1993.

[6] D. M. Pozar, *Microwave Engineering*, 2nd ed. New York: Wiley, 1998.

[7] M. Kirschning and R. H. Jansen, "Accurate wide-range design equations for the frequency-dependent characteristic of parallel coupled microstrip lines," *IEEE Trans. Microw. Theory Tech.*, vol. MTT-32, no. 1, pp. 83–90, Jan. 1984.

[8] ——, "Corrections to 'Accurate wide-range design equations for the frequency-dependent characteristic of parallel coupled microstrip lines'," *IEEE Trans. Microw. Theory Tech.*, vol. MTT-33, no. 3, p. 288, Mar. 1985.

Enrique Márquez-Segura (S'93–M'95) was born in Málaga, Spain, in April 1970. He received the Ingeniero de Telecomunicación and Doctor Ingeniero de Telecomunicación degrees from the Universidad de Málaga, Málaga, Spain, in 1993 and 1998, respectively.

In 1994, he joined the Departamento de Ingeniería de Comunicaciones, Escuela Técnica Superior de Ingeniería de Telecomunicación, Universidad de Málaga, where, in 2001, he became an Associate Professor. His current research interests include EM material characterization, measurement techniques, and RF and microwave circuits design for communication applications.

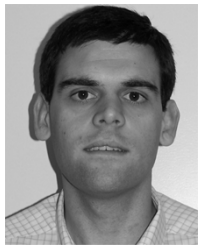

Francisco P. Casares-Miranda (S'05) was born in Granada, Spain, in 1978. He received the Ingeniero de Telecomunicación degree from the Universidad de Málaga, Málaga, Spain, in 2003, and is currently working toward the Ph.D. degree at the University de Málaga.

Since 2004, he has been a Graduate Student and Research Assistant with the Departamento de Ingeniería de Comunicaciones, Escuela Técnica Superior de Ingeniería de Telecomunicación, Universidad de Málaga. His current research is focused on the analysis and applications of left-handed metamaterials.

Mr. Casares was the recipient of a Spanish Ministry of Education and Science scholarship (2004–2008).

Pablo Otero (S'93–M'96) received the Ingeniero de Telecomunicación degree from the Universidad Politécnica de Madrid, Madrid, Spain, in 1983, and the Ph.D. degree from the Swiss Federal Institute of Technology at Lausanne (EPFL), Zürich, Switzerland, in 1998.

After ten years in different Spanish companies, in 1993, he joined the Universidad de Sevilla, Seville, Spain, where he was a Lecturer for two years. In 1998, he joined the Departamento de Ingeniería de Comunicaciones, Escuela Técnica Superior de Ingeniería de Telecomunicación, Universidad de Málaga, Málaga, Spain, where he is currently an Associate Professor. His research interests include EM theory and printed microwave circuits and antennas.

Carlos Camacho-Peñalosa (S'80–M'82) received the Ingeniero de Telecomunicación and Doctor Ingeniero degrees from the Universidad Politécnica de Madrid, Madrid, Spain, in 1976 and 1982, respectively.

From 1976 to 1989, he was with the Escuela Técnica Superior de Ingenieros de Telecomunicación, Universidad Politécnica de Madrid, as Research Assistant, Assistant Professor, and Associate Professor. From September 1984 to July 1985, he was a Visiting Researcher with the Department of Electronics, Chelsea College (now King's College), University of London, London, U.K. In 1989, he became a Professor with the Universidad de Málaga, Málaga, Spain. He was the Director of the Escuela Técnica Superior de Ingenieros de Telecomunicación (1991–1993), Vice-Rector (1993–1994), and Deputy Rector (1994) of the Universidad de Málaga. From 1996 to 2004, he was the Director of the Ingeniería de Telecomunicación. From 2000 to 2003, he was Co-Head of the Nokia Mobile Communications Competence Centre, Málaga, Spain. His research interests include microwave and millimeter solid-state circuits, nonlinear systems, and applied electromagnetism. He has been responsible for several research projects on nonlinear microwave circuit analysis, microwave semiconductor device modeling, and applied electromagnetics.

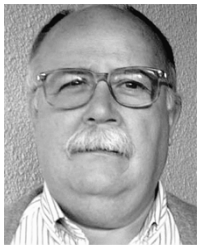

Juan E. Page was born in Madrid, Spain, in 1946. He received the Ingeniero de Telecomunicación and Doctor Ingeniero degrees from the Universidad Politécnica de Madrid, Madrid, Spain, in 1971 and 1974, respectively.

Since 1983, he has been a Professor with the Departamento de Electromagnetismo y Teoría de Circuitos, Universidad Politécnica de Madrid. His activity includes the teaching of EM theory and research in the field of computer-aided design (CAD) of microwave devices and systems.